

Laser Ranging to the Lost Lunokhod 1 Reflector

T. W. Murphy, Jr.¹, E. G. Adelberger², J. B. R. Battat³, C. D. Hoyle⁴, N. H. Johnson¹, R. J. McMillan⁵, E. L. Michelsen¹, C. W. Stubbs⁶, H. E. Swanson²

tmurphy@physics.ucsd.edu

ABSTRACT

In 1970, the Soviet Lunokhod 1 rover delivered a French-built laser reflector to the Moon. Although a few range measurements were made within three months of its landing, these measurements—and any that may have followed—are unpublished and unavailable. The Lunokhod 1 reflector was, therefore, effectively lost until March of 2010 when images from the Lunar Reconnaissance Orbiter (LRO) provided a positive identification of the rover and determined its coordinates with uncertainties of about 100 m. This allowed the Apache Point Observatory Lunar Laser-ranging Operation (APOLLO) to quickly acquire a laser signal. The reflector appears to be in excellent condition, delivering a signal roughly four times stronger than its twin reflector on the Lunokhod 2 rover. The Lunokhod 1 reflector is especially valuable for science because it is closer to the Moon’s limb than any of the other reflectors and, unlike the Lunokhod 2 reflector, we find that it is usable during the lunar day. We report the selenographic position of the reflector to few-centimeter accuracy, comment on the health of the reflector, and illustrate the value of this reflector for achieving science goals.

Subject headings: Moon; Moon, surface; Celestial mechanics

1. Introduction

The Apollo 11 astronauts that landed on the Moon in July, 1969 deployed a retro-reflector intended for lunar laser ranging (LLR). Shortly thereafter, several ground stations, including the Lunar Ranging Experiment (LuRE) at the McDonald Observatory 2.7 m telescope, ranged to the reflector. In November, 1970, the Soviets landed the Lunokhod 1 robotic rover that carried a French-built reflector with a different design but

¹University of California, San Diego, Dept. of Physics, La Jolla, CA 92093-0424

²University Washington, Dept. of Physics, Seattle, WA 98195-1560

³Massachusetts Institute of Technology, Dept. of Physics, Cambridge, MA 02139

⁴Humboldt State University, Dept. of Physics and Astronomy, Arcata, CA 95521-8299

⁵Apache Point Observatory, Sunspot, NM 88349-0059

⁶Harvard University, Dept. of Physics, Cambridge, MA 02318

a comparable expected reflection efficiency. The Soviets (Kokurin 1975) and the French (Calame 1975) both ranged to the reflector during its first lunar night in December of 1970, followed by another success in February, 1971. The LuRE team tried to locate the Lunokhod 1 reflector, and may have seen glimpses of it a time or two, but never enough to pin down its position. Kokurin relates in 1975 that the Lunokhod 1 reflector was seen again in May of 1974, but no details are provided, and the data are not available. The Lunokhod 1 reflector was followed by the the Apollo 14, Apollo 15, and Lunokhod 2 reflectors, arriving in that order. We denote these reflectors as A11, L1, A14, A15, and L2, respectively. The arrival of other reflectors whose coordinates were well known, and which in the case of A15 had much larger effective area, reduced the motivation for spending valuable telescope time on continued searches for L1.

The position of the Lunokhod 1 rover was known to within approximately 5 km (Stooke 2005). This large uncertainty was a problem for LLR, which typically uses a narrow time window to reduce the inevitable background. For example, the Apache Point Observatory Lunar Laser-ranging Operation (APOLLO: Murphy et al. 2008) normally employs a 100 ns detector gate, translating to a one-way range window with a depth of 15 m. Because the lunar surface normal at L1 is angled 50° to the line of sight from Earth, the range window maps to a 20 m wide band on the lunar surface. Positional uncertainty of a few kilometers translates into a vast search space so that detecting the reflector is unlikely. Nonetheless, APOLLO spent a small fraction of its telescope time on favorable nights unsuccessfully exploring the space around the best-guess coordinates of Stooke (2005).

A breakthrough occurred in 2010 March, when the Lunar Reconnaissance Orbiter Camera (LROC: Robinson et al. 2010) obtained a high-resolution image of the Luna 17 landing area that clearly revealed the lander, rover, and rover tracks. The coordinates obtained by the LROC team had an uncertainty of about 100 m (Plescia 2010) and were centered on a region almost 5 km from the previous best estimate. Additionally, laser altimetry from the Lunar Orbiter Laser Altimeter (LOLA: Smith et al. 2010) on board LRO determined the site radius to better than 5 m (Neumann 2010). But it was not possible to know if L1 was correctly oriented toward the Earth. A few unsuccessful ranging attempts were made in late March in unfavorable observing conditions. The first available favorable observing time on 2010 April 22 yielded immediate results, revealing a return that appeared 270 ns later than our prediction. The initial return was surprisingly bright, far surpassing the best-ever return signal from the twin reflector on Lunokhod 2.

2. Observations

Following the initial discovery on April 22, we continued to successfully range to L1 even when seeing conditions were not optimal or when the reflector was illuminated by the sun. We were surprised that L1 remained visible during lunar daylight because, unlike the APOLLO reflectors that are usable in lunar daylight, L2 (L1's twin) cannot be seen when the sun shines on the reflector, even in excellent observing conditions.

Table 1 summarizes our L1 observations, also enumerating range measurements to the other reflectors used to determine the lunar orientation. All sessions, except for 2010 May 24, lasted less than one hour. The

libration offsets in Table 1 incorporate topocentric corrections based on the viewing angle from the Apache Point Observatory (APO) at the time of observation, in effect representing the longitude and latitude of the point on the Moon directly “below” APO. These viewing angles establish the geometry relevant to constraining the position of L1 on the moon. Given the location of L1 on the Moon, the best constraints would arise from maximal librations in the first and third quadrants, i.e., roughly $(7^\circ, 7^\circ)$, and $(-7^\circ, -7^\circ)$. In this case, no observations occupy the third quadrant, and many cluster around similar values. As a result, the centimeter-level position constraints presented here will improve substantially as more observations are made over a broader range of viewing angles.

3. Location of the L1 Reflector

During the first night of observation, the viewing geometry changed enough in 40 minutes to place a weak constraint on the position of the reflector. The error ellipse had an aspect ratio of almost 1000:1, amounting to almost a linear constraint roughly 50 meters long. After 2010 May 5 we could fit for a position accurate to approximately one meter.

Using the L1 range points listed in Table 2 we solved for the coordinates of the L1 reflector. Before the range residuals—the difference between the observation and a prediction based on the Jet Propulsion Laboratory’s DE421 ephemeris—can be used to solve for the reflector position, adjustments for lunar tidal deformation and for Earth and lunar orientations (librations) must be made. Table 2 does not include the initial observations from 2010 April 22 because these observations used a 600 ns detector gate to aid acquisition, rather than the nominal well-calibrated 100 ns gate.

For consistency with DE421, the tidal model assumed second-degree Love numbers $h_2 = 0.0379$ and $l_2 = 0.0105$, so that the tidal displacement vector for a point in the direction \hat{r} from the center of the Moon is

$$\Delta\vec{r} = H \left(\frac{R_0}{R} \right)^3 \left\{ h_2 \hat{r} \left[\frac{3}{2} (\hat{R} \cdot \hat{r})^2 - \frac{1}{2} \right] + 3l_2 (\hat{R} \cdot \hat{r}) \left[\hat{R} - (\hat{R} \cdot \hat{r}) \hat{r} \right] \right\},$$

where \hat{R} is the unit vector from Moon center to the source of the tidal deformation (Earth or Sun), R is the

Table 1: Observation summary

Date	Phase, D	L1 sun elevation	Libration (lon,lat)	A11	L1	A14	A15	L2
2010-04-22	96°	−20°	(−2.9°, 2.7°)	1	4	1	2	—
2010-04-26	150°	18°	(2.1°, 7.3°)	2	1	2	4	—
2010-05-05	263°	33°	(1.9°, −1.9°)	1	2	2	3	2
2010-05-23	118°	−7°	(2.5°, 7.1°)	1	1	1	4	—
2010-05-24	132°	3°	(3.3°, 7.4°)	1	2	1	9	—
2010-06-16	49°	−49°	(−0.8°, 4.2°)	2	3	2	3	2
2010-06-20	102°	−21°	(4.2°, 7.5°)	1	2	2	2	—
2010-08-18	106°	−21°	(7.5°, 4.1°)	1	2	2	3	—

center-to-center distance, R_0 is the time-average distance, and H is the displacement parameter. For Earth-induced tides, $H = 12.89$ m, and $H = 0.074$ m for solar tides. Given the small value for the Love numbers, the tidal amplitude from the Earth is reduced to 0.489 m, and to 2.8 mm for the sun. We applied range offsets to each observation corresponding to the line-of-sight projection of the tidal displacement at the time of observation. Rather than correct to the zero-tide lunar figure, we corrected to the mean, or “static” tidal figure of the tidally-locked Moon, so that corrections were typically less than 0.1 m.

The prediction used in this analysis employs a simple Earth orientation model based on extrapolations of the most recent Earth orientation parameters at the time of observation, resulting in range offsets of several nanoseconds and drift rates approaching 1 ns per hour. Rather than use the best available post-fit Earth orientation parameters, which are accurate to several millimeters, we empirically null Earth orientation effects by subtracting the offset and trend of residuals to the Apollo 15 reflector. The Apollo 15 observations typically bracket observations of the other reflectors and have the most range measurements at the highest precision. This “trend correction” produced the residuals shown in the fifth column of Table 2. Residuals in Table 2 are referenced to the best-fit L1 coordinates. The number of photons used in the reduction represent a subset of the detected photons.

The residuals from the different reflectors differed systematically, indicating errors in the lunar orientation/libration as derived from the DE421 ephemeris. We optimized the lunar orientation by minimizing the residuals of the various reflectors, excluding L1 whose position we were trying to determine. Measurements of the three Apollo reflectors determine the mean range and two orientation angles (the data are insensitive to lunar rotations about the line from the center of the Moon to the observatory). When L2 data are added, the rigid-body fit is over-determined and is found by least-squares minimization, appropriately weighting data points by their measurement uncertainties. The sixth column in Table 2 displays residuals after the lunar orientation corrections are applied to the L1 ranges. In all cases, the orientation corrections were less than 0.15 m on the lunar surface, projecting to less than this in range.

In fitting for an improved reflector position, we evaluated the partial derivatives of the ranges—corrected for tides and orientation—with respect to changes in radius, latitude, and longitude of the reflector from the approximate position determined after 2010 May 5. The partial derivatives were evaluated for each measurement, using the topocentric-corrected libration angle at that time. A least-squares method minimized the chi-squared values of the difference between the measured residual and the predicted location-adjusted range residual from the partial derivatives.

Using all 13 observations in Table 2, we find a position solution with one-sigma errors in the east, north and vertical directions of (0.026, 0.030, 0.025) meters, respectively. In accordance with the usual practice (Amsler et al. 2008), we accounted for the quality of the fit, ($\chi^2/\nu = 2.32$ for $\nu = 10$ degrees of freedom), by multiplying the 1- σ formal errors by $\sqrt{\chi^2/\nu}$. Figure 1 shows the observational constraints on latitude and longitude for a fixed radius.

Table 3 shows our best-fit L1 coordinates referred to the Jet Propulsion Laboratory’s DE421 ephemeris coordinate system for the Moon. Both principal-axis and mean-Earth coordinates are provided, in spherical and Cartesian coordinates. For spherical coordinates, ϕ refers to latitude and λ refers to longitude. The

Table 2: L1 range residuals and uncertainties.

Date	Observation #	# photons used	1σ error (mm)	residual (mm)	
				trend-corrected	libration-corrected
2010-04-26	1	12	19.3	-6.1	-34.4
2010-05-05	2	149	3.6	29.0	-3.0
	3	42	6.9	44.8	12.8
2010-05-23	4	283	2.6	30.3	6.2
2010-05-24	5	23	5.4	32.1	-4.0
	6	90	5.0	29.4	-6.7
2010-06-16	7	104	3.7	21.2	0.0
	8	45	5.3	16.3	-4.9
	9	55	5.4	19.9	-1.2
2010-06-20	10	76	4.5	30.5	-2.4
	11	14	8.6	23.9	-9.0
2010-08-18	12	409	2.5	21.6	3.7
	13	224	2.9	12.9	-5.0

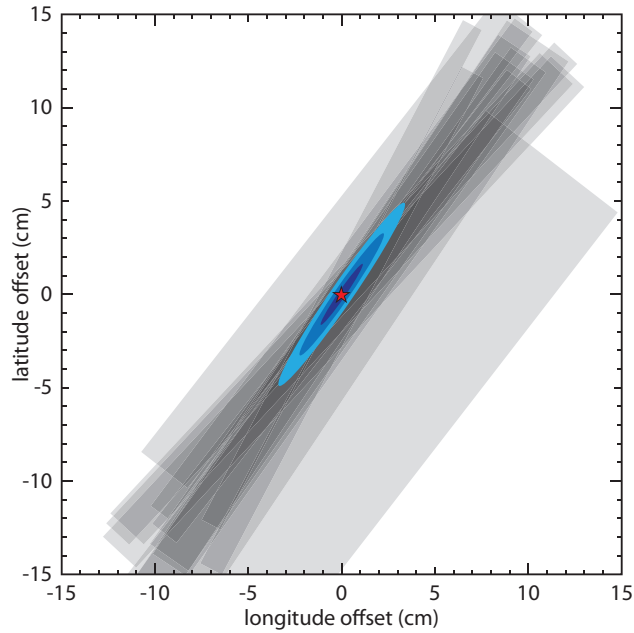


Fig. 1.— Coordinate constraints for the 13 observations in Table 2, confined to the surface at $r = 1734928.72$ m. Gray bands represent individual $1\text{-}\sigma$ constraints, darkening when they overlap, and truncated in length to facilitate individual identification. The joint probability is indicated by the error ellipses, at $1\text{-}\sigma$, $2\text{-}\sigma$, and $3\text{-}\sigma$ levels.

static part of the lunar tide is incorporated in the coordinates for more accurate predictions in the absence of a lunar tidal model. The X -component of the Cartesian set is especially well-determined because this is principally along the direction of the range measurements.

Table 4 includes the coordinates for all five reflectors in the DE421 principal-axis system, repeating coordinates for L1 found in Table 3. The static piece of the lunar tide, given in Table 5, is again incorporated in the coordinates. To obtain the reflector coordinates on the un-deformed Moon, subtract the values in Table 5 from those in Table 4.

4. Reflector Performance

We observed a surprisingly strong signal on APOLLO’s 2010 April 22 discovery of L1, during which we concentrated on verifying the signal by adjusting timing parameters rather than optimizing the signal via pointing adjustments. Nevertheless, we detected 1916 photons from L1 in a 10,000 shot run, compared to 2040 photons from A15 in a 5000 shot run. This suggested that L1 could be expected to deliver at least half the signal strength of the large A15 reflector.

Table 6 compares the normalized observed return rates for the different reflectors. The normalization factor was derived by adding the signal strengths, in photons per shot, for the three Apollo reflectors for the night, and dividing by five. Because the Apollo reflectors have cross-sections in a 1:1:3 ratio, this effectively normalizes the rate to a standard A11/A14 reflector. We find that L1 is approximately four times as bright as L2 when both reflectors are in the dark, and when L1 is illuminated its brightness is comparable to that of L2 in the dark. Table 7 summarizes the results. The Apollo reflectors behave, on average, in their expected 1:1:3 ratio. Averaged over a lunar day, L1 performs comparably to the smaller Apollo arrays, and somewhat better when L1 is in the dark. Our preliminary results are very encouraging for the potential contribution L1 will make to LLR science.

The difference in L1’s and L2’s performance is striking, and as yet unexplained. The LuRE group found that L2 was initially 25% brighter than the A15 reflector. Today, APOLLO typically sees L2 perform at one-tenth the A15 rate. The Apollo reflectors have degraded by as much as a factor of ten since their installation (Murphy et al. 2010), and L2 has clearly degraded more than the Apollo arrays. The fact that L1 performs comparably to the Apollo arrays puts the spotlight on L2, whose rate of degradation appears to be anomalous.

Table 3: L1 Position in DE421 coordinates

Principal Axis, (r, ϕ, λ)	1734928.72±0.03	38.3330784±0.000001	−35.036674 ± 0.000001
Principal Axis, (X, Y, Z)	1114292.387±0.004	−781299.33 ± 0.03	1076058.31±0.03
Mean Earth, (r, ϕ, λ)	1734928.72±0.03	38.3151577±0.000001	−35.007964 ± 0.000001
Mean Earth, (X, Y, Z)	1114959.354±0.004	−780933.94 ± 0.03	1075632.60±0.03

Table 4: Coordinates of the five reflectors, in the DE421 principal-axis frame

Reflector	r (m)	ϕ (deg)	λ (deg)	X (m)	Y (m)	Z (m)
Apollo 11	1735473.105	0.6934308	23.4543026	1591967.923	690698.118	21003.312
Lunokhod 1	1734928.72	38.3330784	-35.036674	1114292.387	-781299.33	1076058.31
Apollo 14	1736336.555	-3.6233280	-17.4971027	1652689.795	-520999.212	-109731.020
Apollo 15	1735477.684	26.1551690	3.6103512	1554679.329	98094.120	765004.914
Lunokhod 2	1734639.201	25.8509889	30.9087373	1339364.890	801870.780	756358.447

Table 5: Static tidal offsets for the five reflectors

Reflector	Δr (m)	$r\Delta\phi$ (m)	$r\Delta\lambda \cos\phi$ (m)
Apollo 11	0.3724	-0.0041	-0.1482
Lunokhod 1	0.0580	-0.1324	0.1497
Apollo 14	0.4196	0.0233	0.1162
Apollo 15	0.3438	-0.1600	-0.0229
Lunokhod 2	0.1926	-0.1173	-0.1610

Table 6: Normalized return rates for the five reflectors; asterisks denote dark conditions

Date	L1 sun elevation	Rate Factor	A11	L1	A14	A15	L2
2010-04-22	-20°	0.0894	0.47	1.70*	1.23*	3.30	—
2010-04-26	18°	0.0383	0.08	0.06	1.24	3.76	—
2010-05-05	33°	0.1770	0.61*	0.23	1.06	3.33	0.17*
2010-05-23	-7°	0.0864	1.12	0.79*	0.56	3.32	—
2010-05-24	3°	0.0116	1.19	1.08	0.61	3.20	—
2010-06-16	-49°	0.0426	0.96*	0.59*	1.08*	2.96*	0.14*
2010-06-20	-21°	0.0077	2.34	1.49*	0.78*	1.88	—
2010-08-18	-21°	0.0410	0.74	1.80*	0.77*	3.49	—

Table 7: Accumulated return rate statistics

Condition	A11	L1	A14	A15	L2
All	0.94	0.97	0.92	3.16	0.155
L1 dark	—	1.27	—	—	—
L1 daylight	—	0.46	—	—	—

The relative expected brightness of the pristine Lunokhod and Apollo reflectors can be calculated as follows. At normal incidence, the triangular-faced Lunokhod corner cubes—measuring 11 cm on a side—have a hexagonal reflecting area of 3493 mm². The 3.8 cm diameter Apollo cubes have a reflective area of 1134 mm² at normal incidence. But the peak intensity of the far-field diffraction pattern from an individual cube scales approximately as the area of the reflector squared. Moreover, the central intensity of an uncoated corner cube relying on total internal reflection—like the Apollo cubes—is only 27% that of a perfect Airy pattern as delivered by a perfectly-coated corner cube. On balance, the central intensity of a single Lunokhod cube will therefore be about 30 times that of an Apollo cube if the reflective coatings on the Lunokhod reflectors operate at 95% efficiency. Taking into account the multiple reflectors—14 in a Lunokhod array vs. 100 in the A11/A14 arrays—one expects the Lunokhod central intensity to be 4.2 times stronger than that from the A11/A14 arrays.

However, the transverse motion of the Moon together with Earth rotation typically impose a velocity aberration on the return of $\delta = 4\text{--}6 \mu\text{rad}$, so that the telescope does not sample the central intensity of the returning far-field diffraction pattern. Because the diffraction pattern from the Lunokhod corner cubes is significantly narrower than that from the Apollo cubes, the Lunokhod cubes suffer a greater loss from velocity aberration. Establishing an effective diameter, $D_{\text{eff}} = 66.7 \text{ mm}$, for the Lunokhod cubes so that $\frac{\pi}{4} D_{\text{eff}}^2 = 3493 \text{ mm}^2$, we find that the Airy pattern intensity at an angle, δ , away from the center is $4J_1^2(x)/x^2$, where $x = \delta\lambda/D_{\text{eff}}$, and $J_1(x)$ is the Bessel function of the first kind, order one. At a wavelength $\lambda = 532 \text{ nm}$, the velocity aberration results in an intensity of 0.2–0.52 times the central intensity, with a typical value (for $\delta = 5 \mu\text{rad}$) of 0.35. Under the same conditions, the Apollo cubes produce an offset return intensity of 0.62–0.81 times the central intensity, with a typical value of 0.72. As a result, the ratio of effective strengths for Lunokhod vs. A11/A14 is only 2.0 rather than 4.2. For 532 nm light at normal incidence, we expect the Lunokhod arrays to deliver twice the return of the A11 and A14 arrays. For the ruby laser used in the initial McDonald operation, the effect is not as severe, so that the expected ratio is 2.55. It is therefore not surprising that the L2 return strength was initially seen to be comparable to that from A15, given that A15 is three times larger than the A11/A14 arrays.

Because the L1 reflector is performing at the expected level relative to the Apollo reflectors, we can comment on the orientation of the reflector. An azimuth offset of 40° or more is enough to eliminate any signal return, while an offset of 21° reduces the signal to one-half its optimal value. It is therefore likely that the rover/reflector are oriented within $\sim 20^\circ$ of the intended azimuth. An elevation angle offset is less likely given the pre-set mechanical mounting angle of the array, together with the fact that the terrain is locally flat aside from craters. The poor performance of L2 cannot easily be attributed to orientation, as the reflector delivered a very strong initial response at its final position.

5. Potential Scientific Impact of Ranging to L1

LLR provides, by determining the shape of the lunar orbit, the most precise tests of many aspects of gravity, including the strong equivalence principle, the constancy of Newton’s constant, geodetic preces-

sion, gravitomagnetism, and the inverse square law (Nordtvedt 1995; Dickey et al. 1994; Williams et al. 1996, 2004; Murphy et al. 2007; Adelberger, Heckel, & Nelson 2003). By determining how the Moon’s orientation responds to known gravitational torques, LLR is also a powerful probe of the internal structure of the Moon (Khan et al. 2004). In both cases, knowing and understanding the Moon’s orientation is vital: we cannot use LLR to locate the Moon’s center of mass without knowing the three-dimensional orientation of the lunar body. In fact, lunar orientation uncertainties are currently a limiting factor in converting high-precision ranging data into tests of fundamental properties of gravity. The orientation of a rigid body is determined by three angles. However, the angle specifying the Moon’s rotation about the axis from its center to the telescope cannot be probed by ranging data as the distances to the reflectors are unchanged by this rotation. Ranges to at least three reflectors are needed to constrain the two relevant angles as well as the distance to the center of the rigid body. The lunar orientation can thus be found whenever the signal strengths permit ranging to all three Apollo reflectors in a single session. APOLLO can often do this because the Apollo reflector efficiencies are roughly independent of the state of solar illumination. Ranges to additional reflectors of course improve the orientation constraints, but more importantly, they now constrain models of the Moon’s tidal deformations that are needed to interpret accurately the ranging data. Ranges to four reflectors provide a single tidal constraint; ranging to a fifth reflector doubles the number of independent constraints on the deformation models. However, this argument underrates the importance of ranging to L1. L2 currently has one tenth the reflection efficiency of A15. Moreover, L2 is unusable in lunar daylight, presumably because of thermal gradients within the corner cubes. Because it is impractical to range near new Moon, L2 is effectively available only one third of the time. Fortunately, as seen in Table 6, L1 is reasonably efficient during lunar daylight and quite efficient during lunar night, so that APOLLO will frequently find four available reflectors—and sometimes five.

The most significant impact of our discovery follows from L1’s location on the Moon. A reflector at the center of the visible face of the Moon contributes only modestly to knowledge of lunar orientation. Libration moves this central reflector as much as 10° from the Earth–Moon line of sight, so that its sensitivity, $\frac{\partial \rho}{\partial \theta} \approx \sin \theta$, may approach 0.17, where θ is the angular displacement of the reflector from the line connecting the ranging station to the center of the Moon. A reflector at the limb of the Moon, by contrast, has a sensitivity of 1.0. L1, located approximately 50° from the Earth–Moon line, is *the closest of the five reflectors* to the lunar limb, and has an orientation sensitivity of 0.77. Table 8 lists the sensitivity for all five reflectors. The nominal values correspond to the sensitivities at the average libration of zero in longitude and latitude. The range indicates extremes for the libration that puts the reflector closest to and farthest from the sub-Earth point on the Moon. Both Lunokhod reflectors offer another advantage over Apollo reflectors because each provides sensitivity to both longitude and latitude librations, whereas the Apollo arrays tend to be principally sensitive to just one of the degrees of freedom.

The L1 reflector is nominally about twice as sensitive to libration as any of the Apollo reflectors. Furthermore, it has a high photon return rate, often greater than of the A11 and A14 reflectors. We therefore expect L1 to become APOLLO’s highest priority reflector following signal acquisition on the largest of the reflectors, A15.

6. Conclusion

We have, for the first time in over three decades, obtained unambiguous LLR returns from the Lunokhod 1 reflector and determined its position with an uncertainty of a few centimeters. We found, to our surprise, that L1 is a much better reflector than its twin L2, so the process that degraded L2 has not had a big effect on L1. L1’s location on the Moon makes it the most sensitive reflector to Moon’s orientation in latitude and longitude. Because of L1’s strategic location and high reflection efficiency that degrades only modestly when it is illuminated by the sun, ranging to this reflector will significantly advance the precision of LLR and the resulting gravitational and lunar science.

T.M. thanks Jim Williams for alerting him to the new LRO images on 2010 March 18, and for providing historical details of L1 ranging efforts. Eric Silverberg related the history of the attempts to locate L1 by the McDonald Observatory. APOLLO is supported by the National Science Foundation (grant PHY-0602507) and the National Aeronautical and Space Administration (NASA; grant NNX-07AH04G). T.M. is also supported by the NASA Lunar Science Institute as part of the LUNAR consortium (NNA09DB30A). Results in this paper are based on observations obtained with the Apache Point Observatory 3.5 m telescope, which is owned and operated by the Astrophysical Research Consortium.

REFERENCES

- Adelberger, E. G., Heckel, B. R., & Nelson, A. E., 2003. Tests of the gravitational inverse-square law. *Annual Review of Nuclear and Particle Science*, 53, 77–121.
- Particle Data Group: Amsler, C., and 170 colleagues, 2008. Review of Particle Physics. *Physics Letters B*, 667, 1–1340 (page 16).
- Calame, O., 1975. Première détermination d’une longue base terrestre par télémétrie laser-Lune et localisation du réflecteur de Lunakhod I. *Comptes Rendus*, 280, 551–554.
- Dickey, J. O., and 11 colleagues, 1994. Lunar Laser Ranging: A Continuing Legacy of the Apollo Program. *Science*, 265, 482.

Table 8: Orientation sensitivity of the reflectors

Reflector	offset (deg)	nominal sensitivity	range	nominal longitude sensitivity	nominal latitude sensitivity
Apollo 11	23.5	0.40	0.27–0.52	0.40	0.01
Lunokhod 1	50.0	0.77	0.65–0.86	0.45	0.51
Apollo 14	17.9	0.31	0.17–0.44	0.30	0.06
Apollo 15	26.4	0.44	0.33–0.55	0.06	0.44
Lunokhod 2	39.5	0.63	0.49–0.76	0.46	0.37

- Khan, A., Mosegaard, K., Williams, J. G., & Lognonne, P., 2004. Does the Moon Posses a Molten Core? Probing the Deep Interior Using results from LLR and Lunar Prospector. *J. of Geophys. Res.– Planets*, 109, E09007.
- Kokurin, Y. L., 1975. Laser Ranging of the Moon. *Proceedings of the P. N. Lebedev Physics Institute*, 91, 161–226.
- Murphy, Jr., T. W., Nordtvedt, K., and Turyshev, S. G., 2007. Gravitomagnetic Influence on Gyroscopes and on the Lunar Orbit. *Phys. Rev. Lett.* 98, 071102.
- Murphy Jr., T. W., and 12 colleagues, 2008. The Apache Point Observatory Lunar Laser-ranging Operation: Instrument description and first detections. *Publ. Astron. Soc. Pacific*, 120, 20–37.
- Murphy Jr., T. W., and 8 colleagues, 2010. Long-term degradation of optical devices on the Moon. *Icarus*, 208, 31–35.
- Neumann, G. A., 24 March 2010, private communication.
- Nordtvedt, K., 1995. The Relativistic Orbit Observables in Lunar Laser Ranging. *Icarus*, 114, 51.
- Plescia J., 24 March 2010, private communication.
- Robinson, M. S., and 22 colleagues, 2010. Lunar Reconnaissance Orbiter Camera (LROC) Instrument Overview. *Space Sci. Rev.*, 150, 81–124.
- Smith, D. E., and 30 colleagues, 2010. The Lunar Orbiter Laser Altimeter Investigation on the Lunar Reconnaissance Orbiter Mission. *Space Sci. Rev.*, 150, 209–241.
- Stooke, P. J., 2005. Lunar Laser Ranging and the Location of Lunokhod 1. *Lunar and Planetary Inst. Technical Rep.*, Vol. 36, 36th Annual Lunar and Planetary Science Conference, ed. S. Mackwell & E. Stansbery, paper 1194.
- Williams, J. G., Newhall, X. X., and Dickey, J. O., 1996. Relativity parameters determined from lunar laser ranging. *Phys. Rev. D*, 53, 6730.
- Williams, J. G., Turyshev, S. G., and Boggs, D. H., 2004. Progress in lunar laser ranging tests of relativistic gravity. *Phys. Rev. Lett.* 93, 261101.